Cellular Signalling 55 (2019) 90–99

Contents lists available at ScienceDirect

Cellular Signalling

journal homepage: www.elsevier.com/locate/cellsig

Liver parenchymal cells lacking Lipocalin 2 (LCN2) are prone to endoplasmic reticulum stress and unfolded protein response

Erawan Borkham-Kamphorst*, Eddy Van de Leur, Ute Haas, Ralf Weiskirchen*

Institute of Molecular Pathobiochemistry, Experimental Gene Therapy and Clinical Chemistry (IFMPEGKC), RWTH Aachen University Hospital, Germany

ARTICLE INFO

Keywords:
ER stress
Unfolded protein response
Hepatocytes
Liver
Inflammation
Lipocalin 2

ABSTRACT

Unfolded protein response (UPR) is an adaptive mechanism allowing the endoplasmic reticulum (ER) to react to an accumulation of unfolded proteins in its lumen, also known as ER stress. The UPR is interconnected with inflammation through several pathways such as reactive oxygen species (ROS) production resulting from the protein folding or alternatively, activation of nuclear factor-κB (NF-κB) and c-Jun N-terminal kinase (JNK) *via* IRE1, or induction of acute phase response (APR). Lipocalin 2 (LCN2) is one of the APR proteins induced under inflammatory conditions and up-regulated during ER stress. Upon incubation of *Lcn2*$^{-/-}$ and wild type (wt) primary hepatocytes with tunicamycin (TM) or thapsigargin (TG) we found the *Lcn2*$^{-/-}$ hepatocytes to react with strong UPR to the ER stress, as evidenced by significantly increased levels of *Grp94*, *Bip* and *Chop* mRNA and protein compared to the wt. TM and TG-treated hepatocytes activated p65 NF-κB and JNK, the pathways that respond to stress stimuli and playing a central role in inflammation and apoptosis, respectively. ER stress further activated and cleaved full-length CREBH/CREB3L3, the hepatocyte specific transcription factor to induce systemic inflammatory responses. Upregulation of the C/EBP homologous protein (CHOP) was very prominent in *Lcn2*$^{-/-}$ hepatocytes and sustained until 48 h, resulting in hepatocyte apoptosis as evidenced by increased cleaved caspase 3. We also explored the UPR of the *Lcn2* null mouse livers in acute intoxication and inflammation stages with a single application of lipopolysaccharide (LPS) or carbon tetrachloride (CCl_4). The *Lcn2* null mice clearly developed stronger UPR in LPS- and CCl_4-induced ER stress compared to the wt. Our findings indicate that the upregulation of LCN2 during ER stress-induced inflammatory responses protects hepatocytes from being overwhelmed by UPR upon liver injury.

1. Introduction

Endoplasmic reticulum (ER) is a membrane-enclosed interconnected organelle responsible for the synthesis, folding, modification and quality control of numerous secretory and membrane proteins [1]. It also is a major site of free calcium storage within the cell [2]. Cells have evolved a unique homeostatic mechanism, termed the unfolded protein response (UPR), to ensure that the ER can adapt to changing environmental and physiological demands of its functions [3]. In mammalian cells, the UPR is controlled by the ER resident trans-membrane proteins like inositol-requiring enzyme-1 (IRE1), protein kinase RNA-like ER kinase (PERK) and activating transcription factor-6 (ATF6) [3].

IRE1 is the most conserved branch of UPR, present from yeast to mammals. In response to ER stress, IRE1 undergoes oligomerization and transautophosphorylation through its kinase domain, resulting in activation of the cytosolic endoribonuclease (RNase) activity. The activated IRE1 removes a small 26 base pair intron from the X-box binding protein-1 (Xbp1) mRNA to produce the spliced Xbp1 (spXbp1) transcription factor [4–6]. This transcription factor regulates expression of the genes involved in protein folding, entry of the proteins to ER, ER-associated protein degradation (ERAD) and biogenesis of ER and Golgi [7].

Abbreviations: APR, acute phase response; ATF4, activating transcription factor 4; ATF6, activating transcription factor 6; BiP/GRP78, binding immunoglobulin protein/glucose-regulated protein 78; CHOP, C/EBP homologous protein; CREBH/CREB3L3, cyclic AMP response element-binding protein H/cyclic AMP-responsive element-binding protein 3-like 3; eIF2α, eukaryotic translation initiation factor 2α; ER, endoplasmic reticulum; ERAD, ER-associated protein degradation; GADD34, growth arrest and DNA damage-inducible protein 34; IRE1, inositol-requiring enzyme 1; JNK, Jun N-terminal kinase; LCN2, Lipocalin 2; NF-κB, nuclear factor-κB; PERK, protein kinase R (PKR)-like endoplasmic reticulum kinase; spXbp1, spliced Xbp1; TG, thapsigargin; TM, tunicamycin; UPR, unfolded protein response; Xbp1, X-box binding protein-1; wt, wild type

* Corresponding authors at: Institute of Molecular Pathobiochemistry, Experimental Gene Therapy and Clinical Chemistry (IFMPEGKC), RWTH-University Hospital, D-52074 Aachen, Germany.

E-mail addresses: eborkham@ukaachen.de (E. Borkham-Kamphorst), rweiskirchen@ukaachen.de (R. Weiskirchen).

https://doi.org/10.1016/j.cellsig.2019.01.001
Received 13 December 2018; Received in revised form 2 January 2019; Accepted 3 January 2019
Available online 04 January 2019
0898-6568/

PERK is a transmembrane protein kinase that, under ER stress conditions, dimerizes and autophosphorylates, favoring the phosphorylation of the eukaryotic translation initiation factor 2α (eIF2α). Phosphorylated eIF2α causes a global translational arrest as a fast adaptive reaction to misfolded or unfolded proteins [8]. It also favors selective translation of activating transcription factor 4 (ATF4) that regulates the expression of genes involved in folding, oxidative stress and amino acid metabolism [9,10].

In response to ER stress, ATF6, a third UPR signal transduction pathway translocates from the ER to the Golgi apparatus where site 1 and site 2 protease cleave the ATF6 luminal and transmembrane domains to release the cytosolic domain [11]. This ATF6 fragment then migrates into the nucleus to transcriptionally up-regulate ER chaperones and ERAD components, thereby enhancing ER protein folding capacity and efficiency of ERAD [12,13]. These initial transcriptional and translational effects of IRE1, PERK and ATF6 signal help cells to adapt to ER stress by enhancing the fidelity of protein folding, increase degradation of unfolded/misfolded proteins and suppress new protein synthesis. Most signaling events downstream of the UPR sensors favor adaptive responses, but if these actions fail to restore ER homeostasis and ER stress persists, UPR signaling consequently triggers proapoptotic programs, many of which are specifically activated through the IRE1 and PERK pathways [14].

The UPR signaling pathways from ER through mitochondria and nucleus suggest that UPR and inflammation are interconnected through various mechanisms that include the production of reactive oxygen species from protein folding processes during intra- and intermolecular disulfide bond formation. It induces also the release of calcium from the ER to the cytosol and mitochondria, the activation of nuclear factor-κB (NF-κB) and Jun N-terminal kinase (JNK) *via* IRE1 and induction of acute phase response (APR) [15].

Several reports have linked UPR induction with production of various pro-inflammatory molecules such as interleukin-8 (IL-8), IL-6, MCP-1 and tumor necrosis factor-α (TNF-α) [16,17]. All three UPR branches have been observed to mediate processes that lead to different inflammatory phenomena, for instance NF-κB, one of the central molecular mediators of inflammation. Recent studies have shown that all major branches of UPR induce activation and nuclear translocation of NF-κB [15] which then induces transcription of various genes coding for pro-inflammatory molecules. Moreover, oxidative stress as a result of ER stress may also contribute to NF-κB activation [18].

UPR signaling pathways can contribute to initiation of the highly complex inflammatory process called acute phase response (APR). The link between APR and ER stress is mainly mediated by two molecules *i.e.* ATF6 and cyclic AMP-responsive element-binding protein H (CREBH) also called cyclic AMP responsive element-binding protein 3-like 3 (CREB3L3), whereby CREBH/CREB3L3 is mainly expressed in hepatocytes [15,19]. Upon ER stress, ATF6 and CREBH traffic from the ER to the Golgi complex, where they are cleaved to release their functional isoforms. Once these 'activated' fragments of CREBH and ATF6 are formed, they translocate into the nucleus and induce transcription of APR genes, such as C-reactive protein, serum amyloid P (SAP) component and Lipocalin 2 (LCN2).

LCN2 is a 25 kDa secretory glycoprotein belonging to the lipocalin family and is one of the APR proteins that are induced under inflammatory conditions [20,21]. This process commences in the early phases of the innate immune responses, mainly due to the activity of pro-inflammatory cytokines like IL-1, IL-6, and TNF-α [22]. In cultured hepatocytes, LCN2 is up-regulated during ER stress (Suppl. Fig. 1) and inflammatory conditions, including APR. Hepatocytes are the major cell types responsible for the highly elevated serum LCN2 protein levels following bacterial infections [23], whereas the upregulated LCN2 protects hepatocytes from IL-1β-induced stress [24]. We therefore examined the UPR in *Lcn2*$^{-/-}$ hepatocytes in chemically-induced ER stress and UPR in *Lcn2* null mice during acute intoxication and inflammation and found that the lack of LCN2 strongly sensitize to ER stress and UPR.

2. Materials and methods

2.1. Hepatocyte isolation and culturing

Primary hepatocytes were isolated from livers of 8–12 weeks old C57BL/6 and *Lcn2*$^{-/-}$ mice through a two-step *in situ* collagenase perfusion method [25] and cultured on collagen-coated dishes in Hepatozyme-SFM medium (Thermo Fisher Scientific, Schwerte, Germany). The protocol used for hepatocyte isolation was approved by the respective authority, which is the Landesamt für Naturschutz, Umwelt und Verbraucherschutz Nordrhein-Westfalen (LANUV) located in Recklinghausen, Germany. For details, see: https://www.lanuv.nrw.de.

2.2. Tunicamycin and thapsigargin treatment

Primary hepatocytes, 1–2 days upon initial plating, were incubated with fresh medium containing 0.125–2 μg/ml tunicamycin (TM) or 0.0625–2 μM thapsigargin (TG) (#17765 and #T9033, Sigma-Aldrich, Taufkirchen, Germany) for 24 h. Cells were then harvested for RNA and protein extracts, while hepatocytes cultured without TM, TG or with DMSO vehicle served as controls.

2.3. RNA isolation, cDNA synthesis, and qRT-PCR

Total RNA was isolated through QIAzol lysis reagent and RNeasy Mini kits (Qiagen, Hilden, Germany) according to manufacturer's instructions, followed by DNAse digestion and subsequent RNeasy clean up. Primers for amplification were selected from sequences deposited in the GenBank database using the online ProbeFinder Software (Universal Probe Library Assay Design Center, Roche Diagnostics, Mannheim, Germany). First-strand cDNA was synthesized from 1 μg RNA in 20 μl volume using SuperScript™ II reverse transcriptase and random hexamer primers (Invitrogen, Life Technologies, Darmstadt, Germany). For quantitative real-time PCR (qRT-PCR), cDNA derived from 50 ng RNA was amplified in 25 μl volume using SYBR® GreenER™ qPCR SuperMix Universal for ABI PRISM® (Invitrogen). PCR conditions were set to 50 °C for 2 min, 40 cycles of 95 °C for 15 s, and 60 °C for 1 min. All primers used in this study are given in Supplementary Table 1.

For conventional polymerase chain reaction (PCR), cDNA was amplified accordingly and subjected to the following cycle conditions: 30 s denaturation at 95 °C, 30 s annealing at 57 °C (Xbp1 #30 cycles) or 60 °C (GAPDH #20 cycles), and 1 min extension at 72 °C. Amplified PCR products were separated on 3% agarose gels for separation of spXbp1 (179 bp) from unspliced Xbp1 (205 bp).

2.4. SDS-PAGE and Western blot analysis

Cell lysates were prepared using RIPA buffer containing 20 mM Tris-HCl (pH 7.2), 150 mM NaCl, 2% (*w/v*) NP-40, 0.1% (w/v) SDS, 0.5% (w/v) sodium deoxycholate and the Complete™-mixture of proteinase inhibitors (Roche). Equal amounts of cellular protein extracts or supernatants were diluted with Nu-PAGE™ LDS electrophoresis sample buffer with DTT as reducing agent, heated at 95 °C for 10 min, and separated in 4–12% Bis-Tris gradient gels, using MOPS or MES running buffers (all from Invitrogen). Proteins were electroblotted onto nitrocellulose membranes (Schleicher & Schuell BioScience GmbH, Dassel, Germany) and equal loading was shown in Ponceau S stain. Subsequently, non-specific binding sites were blocked in Tris-buffered saline (TBS) containing 5% (*w/v*) non-fat milk powder. All antibodies (Supplementary Table 2) were diluted in 2.5% (w/v) non-fat milk powder in TBS. Primary antibodies were visualized using horseradish peroxidase conjugated anti-mouse-, anti-rabbit- or anti-goat IgG (Santa Cruz Biotech, Santa Cruz, CA) and the SuperSignal chemiluminescent

substrate (Pierce, Bonn, Germany).

2.5. Animal experiments, specimen collections and serum analytics

All animal protocols complied with the guidelines for animal care approved by the German Animal Care Committee as mentioned previously for primary hepatocyte isolation. To induce acute hepatic intoxication and inflammation in mice, we used 6–8 week-old C57BL/6 wild type (wt) and *Lcn2*$^{-/-}$ mice [26], subjected to either (i) a single intraperitoneal (i.p.) injection of 0.8 ml/kg body weight CCl_4 diluted in mineral oil for 48 h or (ii) single dose i.p. of LPS (2.5 mg/kg) for 2 and 6 h, respectively. Blood samples for liver function tests were taken after respective times and liver specimens from sacrificed animals were snap frozen in liquid nitrogen for protein and RNA isolation. Frozen tissue section were preserved with Tissue-Tek (Sakura Finetek Europe B. V., Alphen aan den Rijn, The Netherlands) in ice-cold 2-methylbutane (Roth, Karlsruhe, Germany) and kept at -80 °C, or fixed in 4% buffered paraformaldehyde for histology. Routine serum biochemical parameters (aspartate transaminase, AST; alanine aminotransferase, ALT) were measured in the Laboratory Diagnostic Centre of the University Hospital Aachen using the Modular Pre-Analytics (MPA) system (Roche Diagnostics, Mannheim, Germany).

2.6. Oil Red O staining

For Oil red O staining, we used a protocol previously published [27]. In brief, the air-dried and thawed frozen sections were fixed in 4% paraformaldehyde solution for 15 min and excess formaldehyde was removed by three rinses in deionized water. Subsequently, the sections were immersed in the Oil Red O (Sigma-Aldrich) working solution, solubilized in isopropanol, for 30 min at room temperature. Thereafter, the sections were washed 3 times with deionized water and counterstained briefly in hematoxylin solution (DAKO, Hamburg, Germany) to visualize nuclei. The sections were rinsed with running tap water for 10 min and mounted with PermaFluor aqueous mounting solution (Thermo Scientific).

2.7. Bodipy staining

Cultured hepatocytes on sterile glass coverslips were fixed with 4% paraformaldehyde solution for 15 min, and excess formaldehyde was removed by three rinses in phosphate buffered saline (PBS). Cells were covered with 50 µM BODIPY™ 493/503 (ThermoFisher Scientific) in PBS for 30 min at room temperature. Thereafter cells were washed 3× with PBS and DAPI staining was performed by using the Vectashield mounting medium with DAPI (DAKO). Digital imaging was obtained from Nikon Eclipse E80i microscope.

2.8. Repetition and statistics

All *in vitro* experiments depicted were done at least three times. Animal experiments were done with groups of two (controls) to five (treatment) animals per group. Statistical data analysis was performed using the Student *t*-test for comparison of groups to the control. Probability values given are $p < .05$ (*), $p < .01$ (**), and $p < .001$ (***), respectively.

3. Results

3.1. Lcn2$^{-/-}$ hepatocytes react strongly to tunicamycin-induced ER stress

Cultured primary hepatocytes incubated with 0.125 to 2 µg/ml of TM for 24 h showed increased levels of spXbp1 mRNA expression compared to wt control hepatocytes (Fig. 1A). Quantitative RT-PCR confirmed significantly increased binding-immunoglobulin-protein (Bip), 94 kDa glucose-regulated-protein (Grp94) and C/EBP-homologous-protein (Chop) mRNA in *Lcn2*$^{-/-}$ hepatocytes (Fig. 1B). Western blot results showed increased levels of BiP and GRP94 in *Lcn2*$^{-/-}$ hepatocytes, while IRE1α was not significant different compared to hepatocytes obtained from wt mice. Surprisingly the levels of phosphorylated eIF2α showed lower quantities than those obtained in control hepatocytes, but remained slightly higher in *Lcn2*$^{-/-}$ hepatocytes than in wt cells. However, the downstream of PERK-eIF2α signaling pathways, ATF4 and CHOP, were strikingly high in *Lcn2*$^{-/-}$ hepatocytes. LCN2 protein increased slightly with shifting molecular weight in TM-stimulated wt cells due to TM inhibited glycosylation [28] (Fig. 1C). Additionally, ER stress activated and cleaved full length CREBH/CREB3L3, the hepatocyte specific transcription factor necessary to induce systemic inflammatory responses [15] showed lowered expression in both wt and *Lcn2*$^{-/-}$ hepatocytes after incubation with TM (Fig. 1C, Suppl. Fig. 2). TM-treated hepatocytes further activated p65 NF-κB and JNK, the pathways that respond to stress stimuli and playing central roles in inflammation and apoptosis. Furthermore, cytochrome *c* levels in *Lcn2*$^{-/-}$ hepatocytes were markedly increased compared to wt controls (Fig. 1D, Suppl. Fig. 2).

3.2. Tunicamycin-treated hepatocytes induced hepatocyte apoptosis

Upon 24 h TM incubation, the well-recognized proapoptotic factor CHOP showed very high expression in *Lcn2*$^{-/-}$ hepatocytes (*cf.*Fig. 1C). However, we were unable to detect the apoptotic marker cleaved caspase 3 (data not shown). After prolongation of the TM incubation period to 48 and 72 h, we found the ER stress parameters to remain high. In particular, levels of spXbp at 48 h, the ER chaperones Bip and Grp94, the apoptotic enhancers *Chop* and *Trib3* mRNA were all higher in *Lcn2*$^{-/-}$ hepatocytes at 48 h (Fig. 2A, B). *Ero1l* mRNA however was only marginally upregulated in hepatocytes treated with TM for 24 and 48 h (Fig. 2B). Western blot also confirmed the higher levels of BiP, GRP94, IRE1α and ATF4 (Fig. 2C, Suppl. Fig. 3). CHOP remained significantly high in *Lcn2*$^{-/-}$ hepatocytes at 48 h but declined upon 72 h with simultaneous LCN2 protein accumulation in wt hepatocytes. The phosphorylated and total eIF2α and p21/Cip1 were lower than in non-TM-treated hepatocytes, but showed significant ATF6 and CREB3L3 activation as evidenced by the low levels of full-length proteins (Fig. 2C, Suppl. Fig. 3). Phosphorylated p65 NF-κB increased significantly in *Lcn2*$^{-/-}$ hepatocytes, while TNF receptor-associated factor 2 (TRAF2) and p-JNK were reduced after TM treatment (Fig. 2D, Suppl. Fig. 3). Bcl-xL and Bcl2 levels were diminished with increased Bax and Cytochrome c proteins, resulting in increased cellular apoptosis as evidenced by elevated quantities of cleaved caspase 9 and 3 in *Lcn2*$^{-/-}$ hepatocytes compared to wt hepaytocytes (Fig. 2D, Suppl. Fig. 3).

3.3. Lcn2$^{-/-}$ hepatocytes react strongly to thapsigargin-induced ER stress

In cultured hepatocytes incubated with 62.5 to 1000 nM TG for 24 h, only the highest dose of 1000 nM TG induced generation of spXbp1) mRNA (Fig. 3A). The lack of LCN2 produced higher amounts of *Bip*, *Grp94* and *Chop* mRNA when compared to wt hepatocytes (Fig. 3B). Also, the levels of BiP, ATF6 and CHOP proteins were found higher in *Lcn2*$^{-/-}$, while IRE1α was slightly lower compared to the wt cells. Although eIF2α phosphorylation was decreased after TG stimulation, it induced CHOP protein (Fig. 3C, Suppl. Fig. 4). Activation of NF-κB (p-p65), JNK MAPK (p-JNK) was higher in *Lcn2*$^{-/-}$ combined with slightly increased Bcl-xL, Bax and Cytochrome c, while cleaved caspase 3 was not detectable (Fig. 3D, Suppl. Fig. 4).

3.4. Lcn2 null mice developed stronger UPR in lipopolysaccharide (LPS)-induced ER stress than wild type mice

LPS-induced acute inflammation in liver induced by application of 2.5 µg/g body weight induced formation of spXbp1 within 2 h upon LPS

application (Fig. 4A), while the mRNA levels of *Bip*, *Grp94* and *Chop* increased after 6 h, especially in *Lcn2*$^{-/-}$ animals (Fig. 4B). The increase in protein amounts of BiP, p-eIF2α, CHOP, p21/Cip1 and cleaved caspase 3 was confirmed in liver protein extracts prepared after 6 h of LPS injection (Fig. 4C, Suppl. Fig. 5). However, only BiP showed higher levels in livers of *Lcn2*$^{-/-}$ animals when compared to wt controls. After 6 h of LPS stimulation, the levels of GRP94 and IRE1α effectively declined. On the contrary, ATF6 and CREBH/CREB3L3 were activated and cleaved significantly after 2 and 6 h but returned to normal after 24 h. LCN2 protein expression and accumulation was significantly up-regulated in wt mice after LPS challenge at all time points tested (Fig. 4C).

Based on our previous findings demonstrating that *Lcn2* null mice exhibit high amounts of hepatic fat droplets [29,30], we next analyzed liver specimen by Oil Red O stain. This analysis revealed that LPS stimulation provoked an unexpected increase of lipid droplet formation in the livers, which was more profound in *Lcn2* null mice (Fig. 4D).

3.5. *Lcn2* null mice show intensified UPR after acute CCl_4 intoxication

A single application of CCl_4 for 48 h failed to induce formation of spXbp1 in the liver (Fig. 5A), while upregulation of *Bip*, *Grp94* and *Chop* mRNA was only found in *Lcn2*$^{-/-}$ mice (Fig. 5B). The ER stress marker

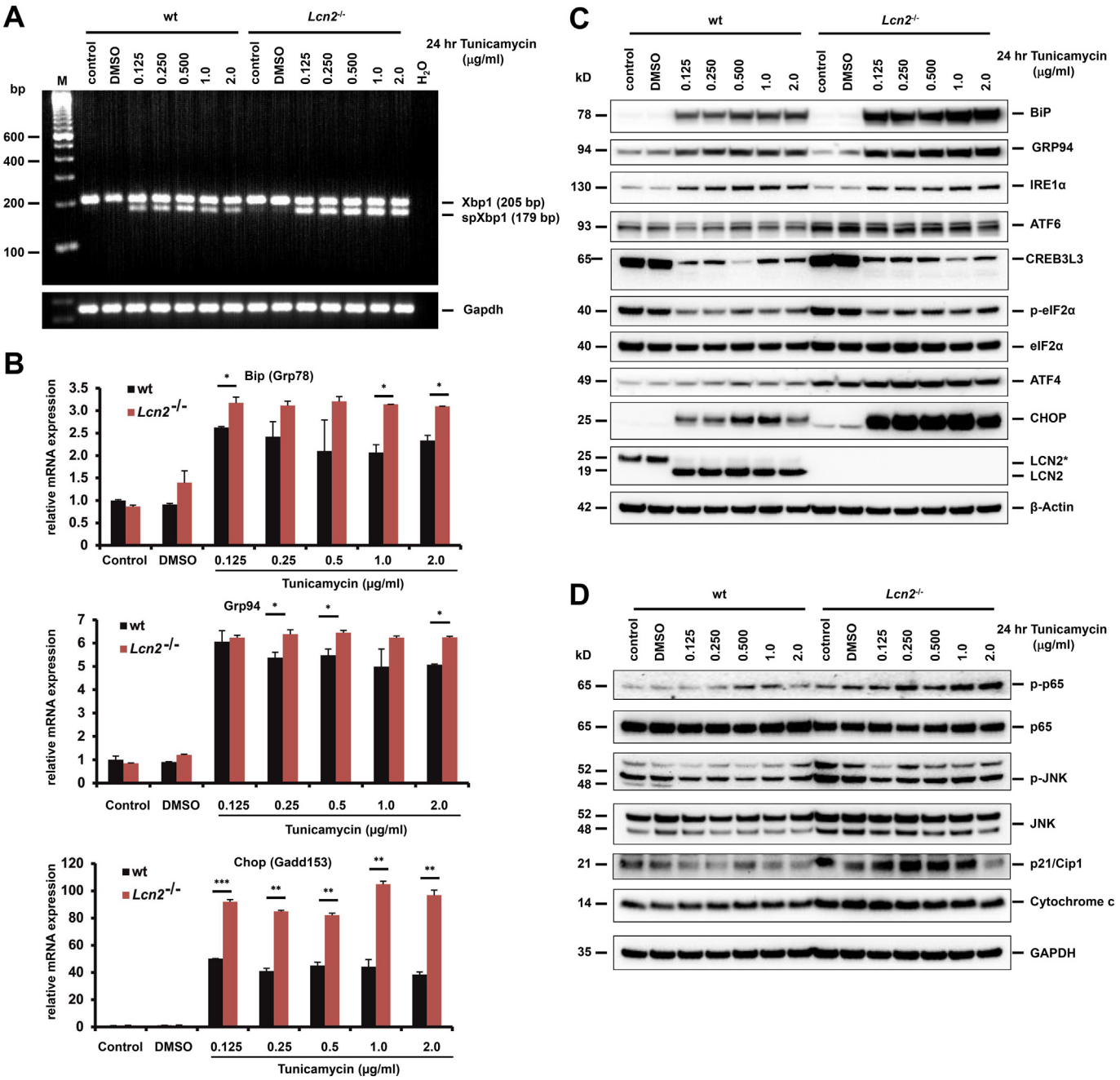

Fig. 1. Twenty four hours tunicamycin-induced ER stress in wt and *Lcn2*$^{-/-}$ hepatocytes. (A) Semi-quantitative PCR depicting unspliced and spliced Xbp1 (spXbp1) mRNA. (B) qRT-PCR showing the ER stress-markers *Bip*, *Grp94*, *Chop* mRNA. Probability values of ≤0.05, ≤ 0.01, and $p < .001$ are marked by (*), (**), or (***), respectively. (C) Western blots of ER stress marker proteins BiP, GRP94, IRE1α, ATF6, p-eIF2α, ATF4, and CHOP. TM-induced ER stress activated and cleaved CREBH/CREB3L3 and induced LCN2 production. TM further inhibited LCN2 glycosylation as evidenced by a shift in molecular weight, with β-actin as a loading control. (D) TM induced p65 NF-κB and JNK MAPK activation along with increased p21/Cip1 and Cytochrome c in *Lcn2*$^{-/-}$ hepatocytes, more than in wt. GAPDH was used as loading controls and Western blot quantifications are shown in Suppl. Fig. 2.

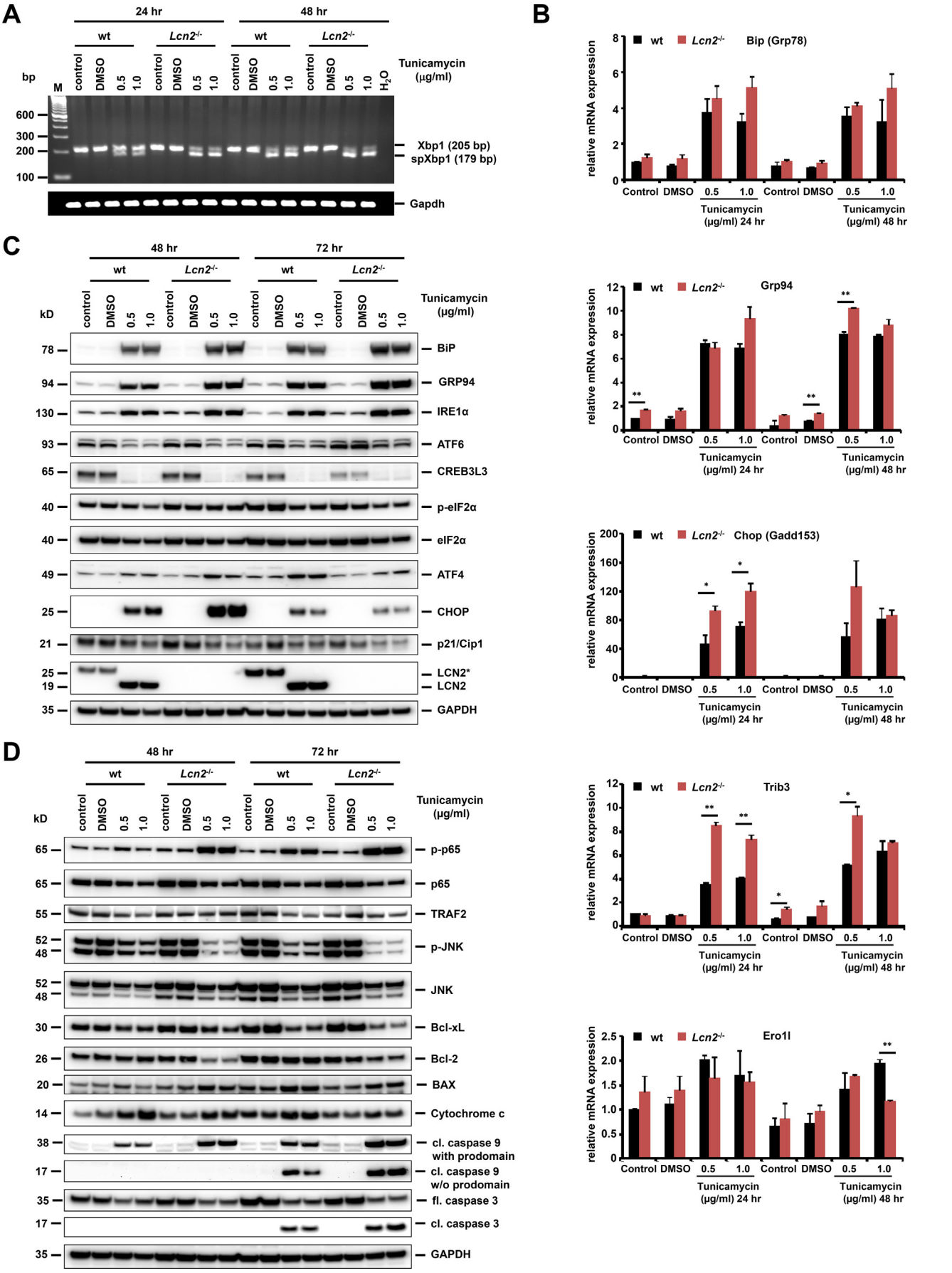

(caption on next page)

Fig. 2. Tunicamycin-induced hepatocyte apoptosis. (A) Semi-quantitative PCR showing un-spliced and spliced Xbp1 (spXbp1) mRNA in hepatocytes cultured in the presence of TM for 24 and 48 h. (B) qRT-PCR of the ER stress-markers *Bip*, *Grp94*, *Chop*, *Trib3* and *Ero1l* mRNA in hepatocytes cultured in the presence of TM for 24 and 48 h. Probability values of ≤0.05 and ≤ 0.01 are marked by (*) or (**), respectively. (C) Western blot analysis of ER stress marker proteins BiP, GRP94, IRE1α, ATF6, p-eIF2α, eIF2α, ATF4, and CHOP. Please note the accumulation of glycosylated and non-glycosylated LCN2 proteins in wt hepatocytes cultured for prolonged time intervals in the presence of TM. GAPDH was used as loading controls. (D) Western blot analysis of p65 NF-κB, TRAF2, JNK MAPK, Bcl-xL, Bcl-2, BAX, Cytochrome c, cleaved caspase 9 (with and w/o prodomain) and caspase 3 (full-length and cleaved). GAPDH was used as loading control. Western blot quantifications are shown in Suppl. Fig. 3.

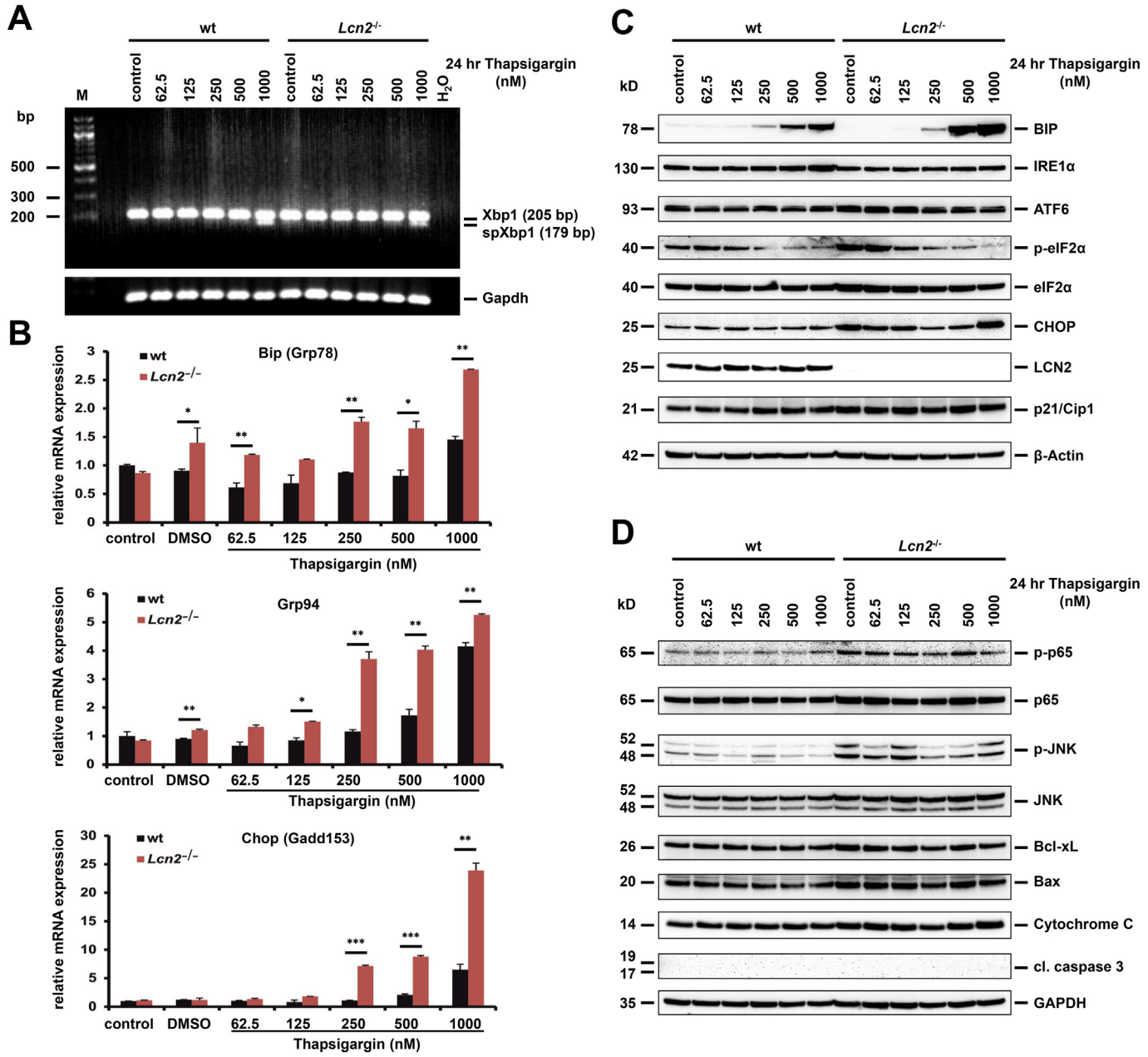

Fig. 3. Twenty-four hours thapsigargin-induced ER stress in wild type and *Lcn2*$^{-/-}$ hepatocytes. (A) In semi-quantitative PCR, only the highest dose (1000 nM) showed spliced Xbp1 (spXbp1) mRNA. (B) qRT-PCR depicting the ER stress-markers *Bip*, *Grp94*, *Chop* mRNA. Probability values of ≤0.05, ≤ 0.01, and p < .001 are marked by (*), (**), or (***), respectively. (C) Western blot analysis of ER stress marker proteins reflecting increased BiP, ATF6, p-eIF2α, eIF2α, CHOP and p21/Cip1 levels in *Lcn2*$^{-/-}$ hepatocytes, while showing slightly decreased IRE1α. In this analysis, β-actin was used as loading control. (D) Western blot analysis showing the *Lcn2*$^{-/-}$ hepatocytes to possess higher levels of p-p65, p65, p-JNK, JNK, Bcl-xL, Bax and Cytochrome c, while no cleaved caspase 3 was detected. GAPDH served as loading control. Western blot quantifications are shown in Suppl. Fig. 4.

proteins BiP, GRP94, ATF6, CHOP and p21/Cip1 were significant higher after CCl_4 challenge in *Lcn2* null mice than in wt animals. Moreover, IRE1α, p-eIF2α, Cytochrome c and cleaved caspase 3 were increased after CCl_4 injection (Fig. 5C, Suppl. Fig. 5). Serum AST and ALT levels increased in CCl_4-injected mice and showed markedly higher values in *Lcn2* null mice (Fig. 5D). As previously reported, the *Lcn2* null mice developed spontaneous steatosis [29,30], while CCl_4 intoxication significantly enhanced steatosis particularly in *Lcn2* null mice (Fig. 5E).

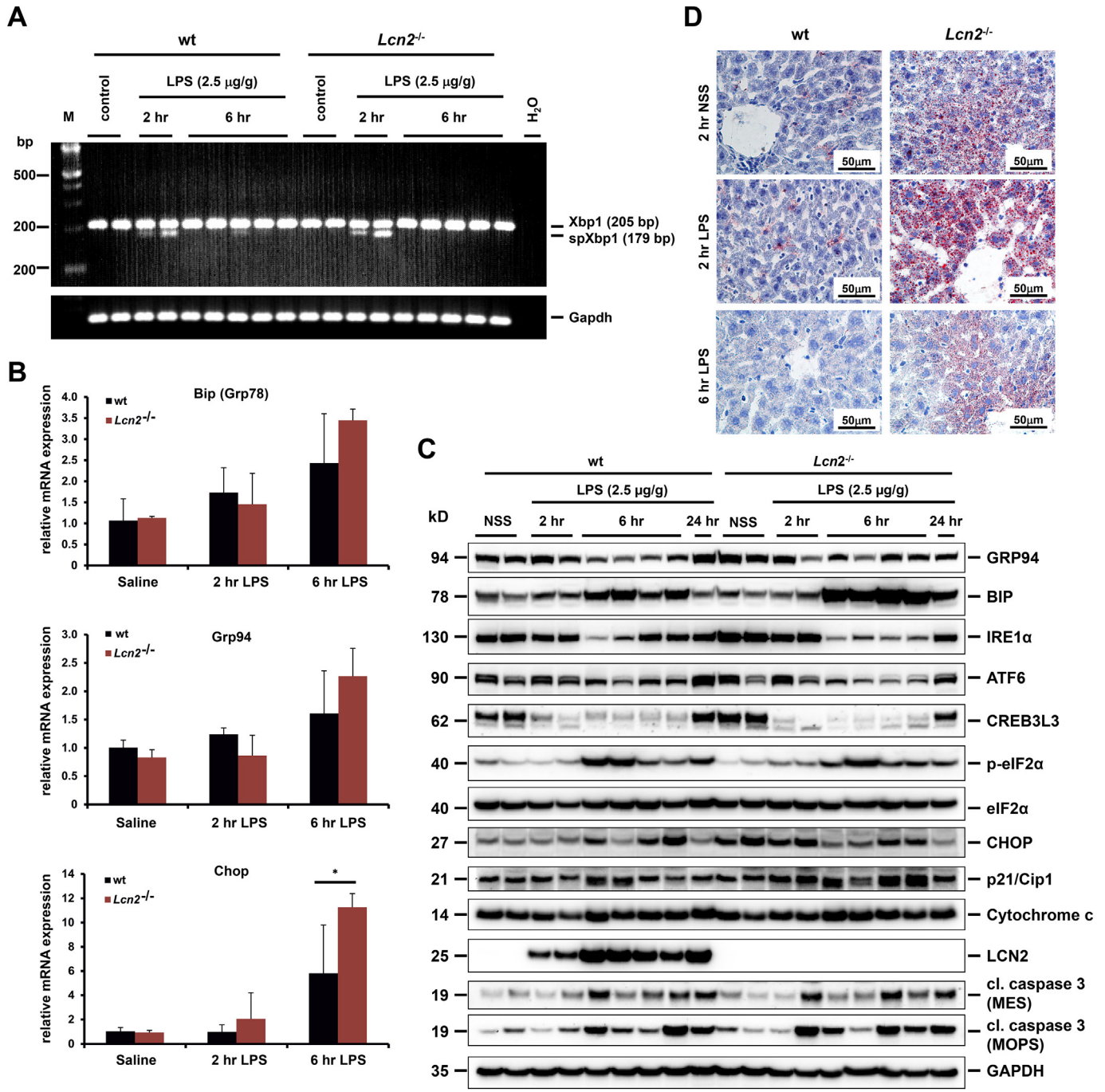

Fig. 4. UPR in lipopolysaccharide-induced ER stress in wild type and *Lcn2* null mice. (A) Semi-quantitative PCR showed Xbp1 splicing 2 h after LPS application. (B) qRT-PCR showing increased ER stress-markers *Bip*, *Grp94*, *Chop* mRNA upon 6 h LPS injection. Probability values of ≤0.05 are marked by (*). (C) Western blot analysis showing increased BiP, p-eIF2α, CHOP, p21/Cip1, Cytochrome c and cleaved caspase 3 after 6 h LPS injection with decreased GRP94, IRE1α, ATF6 and CREB3L3 levels that returned to normal levels at 24 h. Upregulation of BiP and CHOP was higher in $Lcn2^{-/-}$ mice compared with wt animals. Accumulation of LCN2 protein was evidenced in LPS injected wt animals. GAPDH was used as loading control. (D) Oil red O staining showing increased amounts of liver lipid droplets in $Lcn2^{-/-}$ mice upon 2 and 6 h LPS application. (For interpretation of the references to colour in this figure legend, the reader is referred to the web version of this article.)

4. Discussion

ER stress occurs when the ER functions in an environment that lies outside of its normal physiological range. Pharmacological agents such as TM and TG induce ER stress through altered protein glycosylation or by changing ER calcium content, respectively. We applied TM or TG in $Lcn2^{-/-}$ and wt cultured primary hepatocytes and evaluated the ER stress response and UPR. $Lcn2^{-/-}$ hepatocytes responded with stronger UPR reaction than wt hepatocytes as evidenced by a significant higher amount of spXbp1 mRNA (Fig. 1A) along with up-regulation of the UPR markers BiP, GRP94 and CHOP (Fig. 1B and C). Surprisingly, the phosphorylation levels of eIF2α in respective cells were lower than in control cultures or cells that received the DMSO vehicle (Fig. 1C). The reason might be due to the 24 h incubation time, which already declined eIF2α phosphorylation (not shown) and because of hepatocytes response to ER stress immediately decreasing protein production, while

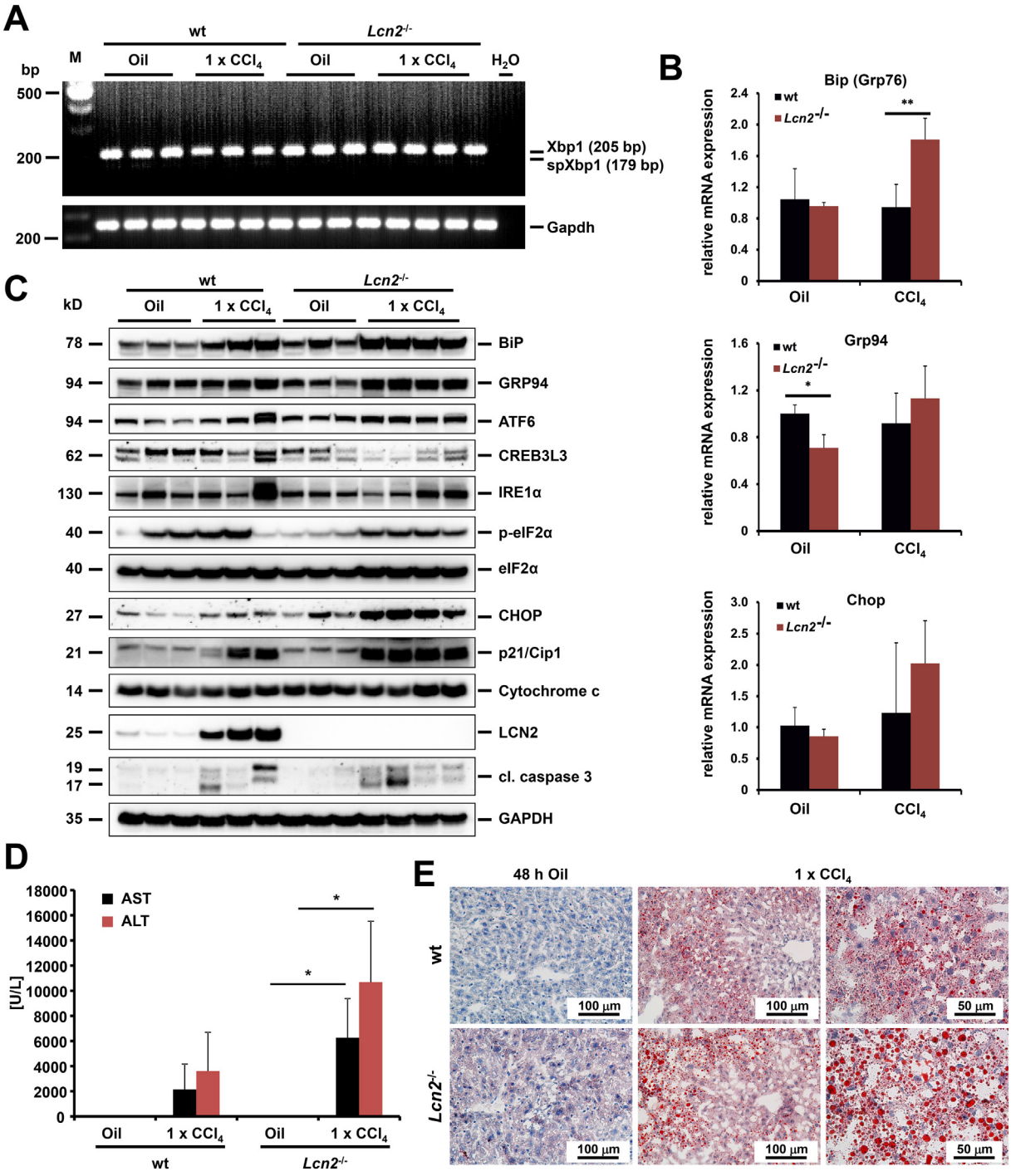

Fig. 5. ER stress markers after single dose CCl_4 application. (A) Semi-quantitative PCR showed no Xbp1 splicing upon 48 h CCl_4 injection. (B) qRT-PCR showing the ER stress-markers *Bip*, *Grp94*, Chop mRNA to increase in livers of *Lcn2*$^{-/-}$ mice. Probability values of ≤0.05 and ≤ 0.01are marked by (*) or (**), respectively. (C) Western blot analysis showing increased BiP, GRP94, ATF6, IRE1α, p-eIF2α, CHOP, p21/Cip1, Cytochrome c and cleaved caspase 3 upon CCl_4 injection. Levels of GRP94, BIP, p21/Cip1 and CHOP were higher in *Lcn2*$^{-/-}$ mice, with markedly decreased full-length CREB3L3 protein quantities compared to wt controls. The quantity of LCN2 protein production after CCl_4 injection was significantly increased in livers wt animals. GAPDH was used as loading control. (D) Serum AST and ALT were measured in wt and *Lcn2*$^{-/-}$ mice 48 h after a single CCl_4 injection. Probability values of ≤0.05 are marked by (*). (E) Oil Red O staining showed an increased amount of liver lipid droplets in *Lcn2*$^{-/-}$ mice upon 48 h CCl_4 injections as compared to wt animals. (For interpretation of the references to colour in this figure legend, the reader is referred to the web version of this article.)

producing huge amount of APR proteins. Downstream of PERK-eIF2α signaling we observed increased ATF4 and subsequently extremely high CHOP expression (Fig. 1C). ATF4 activates transcription of pro-survival genes such as a cyclin-dependent kinase inhibitor p21/Cip1 and induces the pro-apoptotic gene CHOP, which in fact is highly dependent on ATF4 [31]. This phenomenon is also observed in JNK MAPK signaling, but the actual levels of JNK activation at 24 h of TM and TG incubation remained higher in *Lcn2*$^{-/-}$ hepatocytes compared to the wt (Fig. 1D). *Lcn2*$^{-/-}$ hepatocytes possessed higher levels of full-length ATF6 and CREBH/CREB3L3 in the control cultures and DMSO vehicle (Fig. 1D). Under ER stress conditions resulting from TM and TG incubation these two molecules are activated through site 1 and site 2 proteases in Golgi

resulting in markedly decreased full-length proteins. The processed ATF6 fragment then translocates to the nucleus, where it activates transcription of ER stress responsive genes, while CREBH/CREB3L3 induces expression of genes responsible for the systemic inflammatory response [19].

CHOP plays an important role in ER stress-induced apoptosis in a number of disease models, including ethanol-induced hepatocyte injury [32]. On the other side, 24 h treatment with TM or TG were unable to induce cleaved caspase 3, the executive caspase and indicator of cellular apoptosis, in hepatocytes (Fig. 3D). However, upon prolonged TM incubation for 72 h, both *Lcn2*$^{-/-}$ and wt hepatocytes undergone apoptosis with higher caspase 3 and 9 activation, while the observed increase in these caspases was more pronounced in *Lcn2*$^{-/-}$ hepatocytes (Fig. 2D). One mechanism of CHOP-induced apoptosis is suppression of the pro-survival protein Bcl-2. Such a correlation among CHOP expression, oxidative stress, apoptosis and downregulation of Bcl-2 was demonstrated in a CHOP-transfected rat fibroblast cell line [33]. Additionally, genetic restoration of Bcl-2 rescued the CHOP-transfected cells from both oxidative stress and apoptosis [33]. Our findings showed diminished amounts of Bcl-xL and Bcl-2 proteins after TM treatment that were accompanied by a very high CHOP expression in *Lcn2*$^{-/-}$ hepatocytes (Fig. 2D). Bax and Cytochrome c levels showed upregulation, whereas Bax increased with ER stress in a CHOP-dependent manner (Fig. 2D).

Another pathway by which CHOP mediates apoptosis is *via* the growth arrest and DNA damage-inducible protein 34 (GADD34), which is involved in the control of protein translation. GADD34 promotes dephosphorylation of phosphorylated eIF2α, thus restores protein translation, representing another pro-apoptotic mechanism of prolonged CHOP expression [31,34,35]. This may be the cause of decreased phosphorylated eIF2α in our experiments. Additionally, CHOP is also known to induce molecules directly implicated in apoptosis such as death receptor 5 (DR5 also known as TRAIL-R2) [36], tribbles pseudokinase 3 (Trib3) [37], and endoplasmic reticulum oxidoreductin 1-α (Ero1l) [38]. We found only modest cleaved caspase 8 (data not shown), but high levels of *Trib3* mRNA in *Lcn2*$^{-/-}$ with modestly increased Ero1l (Fig. 2B).

UPR is activated by several factors, including nutrient excess and deprivation, reducing agents, oxidative stress, bacterial and viral infections, and also bacterial toxins. For our *in vivo* models of ER stress, we chose acute liver injury induced by single application of LPS or CCl_4. LPS-treated mice showed UPR in early stages as evidenced by generation of spXbp1 mRNA after challenge for 2 h (Fig. 4A), while expression of the ER chaperones BiP and GRP94, and CHOP appeared at later stages (Fig. 4B and C). The protein levels showed increased BiP, p-eIF2α, CHOP and p21/Cip1 with decreased GRP94 and IRE1α (Fig. 4C). In addition, ATF6 and CREB3L3 were activated as shown by markedly decreased full length proteins in *Lcn2*$^{-/-}$ mice compared to the wt, while cleaved caspase 3 showed no difference. This finding is in line with previously reporting that CREBH interacts with ATF6 and works in tandem to activate gene expression of major APR genes such as serum amyloid P component, C-reactive protein [19], and LCN2 [21]. Unexpectedly, LPS application showed to markedly increase hepatocyte fat droplets (Fig. 4D), despite that *Lcn2*$^{-/-}$ liver already contained more fat droplets. This finding seems supported by Xu and colleagues, who reported that CREBH promoted lipid droplet enlargement and triglyceride accumulation in liver [39]. Additionally, TM and TG induce *de novo* lipogenesis and lipid droplet formation in Huh-7, a human hepatoma cell line [40]. This finding was confirmed in TM-treated cultured hepatocytes as we found *Lcn2*$^{-/-}$ hepatocytes to develop more lipid droplets compared to the wt (Suppl. Fig. 6A), in tandem with increased expression of the lipogenic trans-activators including peroxisome proliferator-activated receptor gamma (Pparγ), Pparγ coactivator 1-α (Ppargc1α), and nuclear receptor subfamily 1 group H member 3 (Nr1h3) (Suppl. Fig. 6B). Also increased were components of lipid droplets including cell death-inducing DFFA-like effector c (Cidec), perilipin 2 (Plin2/ADRP), fat storage-inducing transmembrane protein 2 (Fitm2), and key enzymes involved in *de novo* lipogenesis such as acetyl-coenzyme A carboxylase α (Acara) and stearoyl-CoA desaturase 1 (Scd1) (Suppl. Fig. 6B). Chronic or sustained UPR may therefore induce spontaneous liver steatosis in *Lcn2* null mice.

In a 48 h single dose CCl_4 liver intoxication model however we found no spXbp1 mRNA but an elevated expression of BiP, GRP94 and CHOP (Fig. 5). GRP94, ATF6, CHOP and p21/Cip1 were more elevated in *Lcn2* null mice compared to the wt after injection of CCl_4, while the levels of IRE1α, phospho-eIF2α and cleaved caspase 3 were comparable. CREB3L3 activation was significant higher in livers of *Lcn2* null mice when compared with wt animals. The strong UPR corresponded well with more elevated serum liver enzymes AST and ALT in *Lcn2* null mice (Fig. 5D). In addition, liver steatosis was significantly more severe in *Lcn2* null mice compared to control mice (Fig. 5D). The cellular damage found was more severe in hepatocytes lacking LCN2 which may be the result of chronic UPR, especially sustained CHOP expression culminating in hepatocyte apoptosis.

5. Conclusions

In summary, the acute phase protein LCN2 protects hepatocytes through avoiding excessive UPR, resulting in prevention of CHOP-induced hepatocyte apoptosis and chronic ER stress-induced liver steatosis. Chronic or sustained UPR provokes spontaneous liver steatosis in *Lcn2* null mice.

Supplementary data to this article can be found online at https://doi.org/10.1016/j.cellsig.2019.01.001.

Acknowledgements

The authors acknowledge support by the German Research Foundation (SFB/TRR 57, projects P13 and Q3) and from the Interdisciplinary Centre for Clinical Research within the Faculty of Medicine at the RWTH Aachen University (IZKF Aachen, projects O3-1 and O3-9). The funders had no role in study design, data collection and analysis, decision to publish, or preparation of the manuscript. Special gratitude goes to Drs Thorsten Berger and Tak W. Mak, (The Campbell Family Institute for Breast Cancer Research, Ontario Cancer Institute, University Health Network, Departments of Medical Biophysics and Immunology, University of Toronto, Toronto, Canada) who provided *Lcn2* null mice for our study. In addition, the authors acknowledge the help of Sabine Weiskirchen (IFMPEGKC, University Hospital Aachen) in preparing the graphical abstract to this paper.

References

[1] S.S. Cao, R.J. Kaufman, Unfolded protein response, Curr. Biol. 22 (2012) R622–R626, https://doi.org/10.1016/j.cub.2012.07.004.
[2] J.S. So, Roles of endoplasmic reticulum stress in immune responses, Mol. Cell 41 (2018) 705–716, https://doi.org/10.14348/molcells.2018.0241.
[3] C. Hetz, F.R. Papa, The unfolded protein response and cell fate control, Mol. Cell 69 (2018) 169–181, https://doi.org/10.1016/j.molcel.2017.06.017.
[4] C.E. Shamu, P. Walter, Oligomerization and phosphorylation of the Ire1p kinase during intracellular signaling from the endoplasmic reticulum to the nucleus, EMBO J. 15 (1996) 3028e3039.
[5] T.N. Gonzalez, P. Walter, Ire1p: a kinase and site-specific endoribonuclease, Methods Mol. Biol. 160 (2001) 25–36, https://doi.org/10.1385/1-59259-233-3:025.
[6] M. Calfon, H. Zeng, F. Urano, J.H. Till, S.R. Hubbard, H.P. Harding, S.G. Clark, D. Ron, IRE1 couples endoplasmic reticulum load to secretory capacity by processing the XBP-1 mRNA, Nature 415 (2002) 92–96, https://doi.org/10.1038/415092a.
[7] A.H. Lee, N.N. Iwakoshi, L.H. Glimcher, XBP-1 regulates a subset of endoplasmic reticulum resident chaperone genes in the unfolded protein response, Mol. Cell. Biol. 23 (2003) 7448–7459, https://doi.org/10.1128/MCB.23.21.7448-7459.2003.
[8] H.P. Harding, I. Novoa, Y. Zhang, H. Zeng, R. Wek, M. Schapira, D. Ron, Regulated translation initiation controls stress-induced gene expression in mammalian cells, Mol. Cell 6 (2000) 1099–1108, https://doi.org/10.1016/S1097-2765(00)00108-8.
[9] K.M. Vattem, R.C. Wek, Reinitiation involving upstream ORFs regulates ATF4 mRNA translation in mammalian cells, Proc. Natl. Acad. Sci. U. S. A. 101 (2004)

11269–11274, https://doi.org/10.1073/pnas.0400541101.
[10] H.P. Harding, Y. Zhang, H. Zeng, I. Novoa, P.D. Lu, M. Calfon, N. Sadri, C. Yun, B. Popko, R. Paules, D.F. Stojdl, J.C. Bell, T. Hettmann, J.M. Leiden, D. Ron, H.P. Harding, Y. Zhang, H. Zeng, I. Novoa, P.D. Lu, M. Calfon, N. Sadri, C. Yun, B. Popko, R. Paules, D.F. Stojdl, J.C. Bell, T. Hettmann, J.M. Leiden, D. Ron, Mol. Cell 11 (2003) 619–633, https://doi.org/10.1016/S1097-2765(03)00105-9.
[11] K. Haze, H. Yoshida, H. Yanagi, T. Yura, K. Mori, Mammalian transcription factor ATF6 is synthesized as a transmembrane protein and activated by proteolysis in response to endoplasmic reticulum stress, Mol. Biol. Cell 10 (1999) 3787–3799, https://doi.org/10.1091/mbc.10.11.3787.
[12] R. Asada, S. Kanemoto, S. Kondo, A. Saito, K. Imaizumi, The signalling from endoplasmic reticulum-resident bZIP transcription factors involved in diverse cellular physiology, J. Biochem. 149 (2011) 507–518, https://doi.org/10.1093/jb/mvr041.
[13] J. Wu, D.T. Rutkowski, M. Dubois, J. Swathirajan, T. Saunders, J. Wang, B. Song, G.D. Yau, R.J. Kaufman, ATF6α optimizes long-term endoplasmic reticulum function to protect cells from chronic stress, Dev. Cell 13 (2007) 351–364, https://doi.org/10.1016/j.devcel.2007.07.005.
[14] C. Hetz, The unfolded protein response: controlling cell fate decisions under ER stress and beyond, Nat. Rev. Mol. Cell Biol. 13 (2012) 89–102, https://doi.org/10.1038/nrm3270.
[15] K. Zhang, R.J. Kaufman, From endoplasmic-reticulum stress to the inflammatory response, Nature 454 (2008) 455–462, https://doi.org/10.1038/nature07203.
[16] J.C. Duvigneau, A. Luís, A.M. Gorman, A. Samali, D. Kaltenecker, R. Moriggl, A.V. Kozlov, Crosstalk between inflammatory mediators and endoplasmic reticulum stress in liver diseases, Cytokine (2018 Nov 13), https://doi.org/10.1016/j.cyto.2018.10.018 [Epub ahead of print].
[17] J.A. Smith, Regulation of cytokine production by the unfolded protein response; implications for infection and autoimmunity, Front. Immunol. 9 (2018) 422, https://doi.org/10.3389/fimmu.2018.00422.
[18] H. Sies, C. Berndt, D.P. Jones, Oxidative stress, Annu. Rev. Biochem. 86 (2017) 715–748, https://doi.org/10.1146/annurev-biochem-061516-045037.
[19] K. Zhang, X. Shen, J. Wu, K. Sakaki, T. Saunders, D.T. Rutkowski, S.H. Back, R.J. Kaufman, Endoplasmic reticulum stress activates cleavage of CREBH to induce a systemic inflammatory response, Cell 124 (2006) 587–599, https://doi.org/10.1016/j.cell.2005.11.040.
[20] Q. Liu, M. Nilsen-Hamilton, Identification of a new acute phase protein, J. Biol. Chem. 270 (1995) 22565–22570, https://doi.org/10.1074/jbc.270.38.22565.
[21] S. Sultan, M. Pascucci, S. Ahmad, I.A. Malik, A. Bianchi, P. Ramadori, G. Ahmad, G. Ramadori, LIPOCALIN-2 is a major acute-phase protein in a rat and mouse model of sterile abscess, Shock 37 (2012) 191–196, https://doi.org/10.1097/SHK.0b013e31823918c2.
[22] E. Borkham-Kamphorst, F. Drews, R. Weiskirchen, Induction of lipocalin-2 expression in acute and chronic experimental liver injury moderated by pro-inflammatory cytokines interleukin-1β through nuclear factor-κB activation, Liver Int. 31 (2011) 656–665, https://doi.org/10.1111/j.1478-3231.2011.02495.x.
[23] M.J. Xu, D. Feng, H. Wu, H. Wang, Y. Chan, J. Kolls, N. Borregaard, B. Porse, T. Berger, T.W. Mak, J.B. Cowland, X. Kong, B. Gao, Liver is the major source of elevated serum lipocalin-2 levels after bacterial infection or partial hepatectomy: a critical role for IL-6/STAT3, Hepatology 61 (2015) 692–702, https://doi.org/10.1002/hep.27447.
[24] Y. Hu, J. Xue, Y. Yang, X. Zhou, C. Qin, M. Zheng, H. Zhu, Y. Liu, W. Liu, G. Lou, J. Wang, S. Wu, Z. Chen, F. Chen, Lipocalin 2 upregulation protects hepatocytes from IL1-β-induced stress, Cell. Physiol. Biochem. 36 (2015) 753–762, https://doi.org/10.1159/000430135.
[25] E. Borkham-Kamphorst, S. Huss, E. Van de Leur, U. Haas, R. Weiskirchen, Adenoviral CCN3/NOV gene transfer fails to mitigate liver fibrosis in an experimental bile duct ligation model because of hepatocyte apoptosis, Liver Int. 32 (2012) 1342–1353, https://doi.org/10.1111/j.1478-3231.2012.02837.x.
[26] T. Berger, A. Togawa, G.S. Duncan, A.J. Elia, A. You-Ten, A. Wakeham, H.E. Fong, C.C. Cheung, T.W. Mak, Lipocalin 2-deficient mice exhibit increased sensitivity to Escherichia coli infection but not to ischemia-reperfusion injury, Proc. Natl. Acad. Sci. U. S. A. 103 (2006) 1834–1839, https://doi.org/10.1073/pnas.0510847103.
[27] R. Koopman, G. Schaart, M.K. Hesselink, Optimisation of oil red O staining permits combination with immunofluorescence and automated quantification of lipids, Histochem. Cell Biol. 116 (2001) 63–68.
[28] E. Borkham-Kamphorst, E. Van de Leur, S.K. Meurer, E.M. Buhl, R. Weiskirchen, N-Glycosylation of Lipocalin 2 is not required for secretion or exosome targeting, Front. Pharmacol. 9 (2018) 426, https://doi.org/10.3389/fphar.2018.00426.
[29] E. Borkham-Kamphorst, E. van de Leur, H.W. Zimmermann, K.R. Karlmark, L. Tihaa, U. Haas, F. Tacke, T. Berger, T.W. Mak, R. Weiskirchen, Protective effects of lipocalin-2 (LCN2) in acute liver injury suggest a novel function in liver homeostasis, Biochim. Biophys. Acta 1832 (2013) 660–673, https://doi.org/10.1016/j.bbadis.2013.01.014.
[30] A. Asimakopoulou, E. Borkham-Kamphorst, M. Henning, E. Yagmur, N. Gassler, C. Liedtke, T. Berger, T.W. Mak, R. Weiskirchen, Lipocalin-2 (LCN2) regulates PLIN5 expression and intracellular lipid droplet formation in the liver, Biochim. Biophys. Acta 1842 (2014) 1513–1524, https://doi.org/10.1016/j.bbalip.2014.07.017.
[31] E. Szegezdi, S.E. Logue, A.M. Gorman, A. Samali, Mediators of endoplasmic reticulum stress-induced apoptosis, EMBO Rep. 7 (2006) 880–885, https://doi.org/10.1038/sj.embor.7400779.
[32] C. Ji, R. Mehrian-Shai, C. Chan, Y.H. Hsu, N. Kaplowitz, Role of CHOP in hepatic apoptosis in the murine model of intragastric ethanol feeding, Alcohol. Clin. Exp. Res. 29 (2005) 1496–1503, https://doi.org/10.1097/01.alc.0000174691.03751.11.
[33] K.D. McCullough, J.L. Martindale, L.O. Klotz, T.Y. Aw, N.J. Holbrook, Gadd153 sensitizes cells to endoplasmic reticulum stress by down-regulating Bcl2 and perturbing the cellular redox state, Mol. Cell. Biol. 21 (2001) 1249–1259, https://doi.org/10.1128/MCB.21.4.1249-1259.2001.
[34] D. Ron, P. Walter, Signal integration in the endoplasmic reticulum unfolded protein response, Nat. Rev. Mol. Cell Biol. 8 (2007) 519–529, https://doi.org/10.1038/nrm2199.
[35] M.H. Brush, D.C. Weiser, S. Shenolikar, Growth arrest and DNA damage-inducible protein GADD34 targets protein phosphatase 1α to the endoplasmic reticulum and promotes dephosphorylation of the α subunit of eukaryotic translation initiation factor 2, Mol. Cell. Biol. 23 (2003) 1292–1303, https://doi.org/10.1128/MCB.23.4.1292-1303.2003.
[36] H. Yamaguchi, H.G. Wang, CHOP is involved in endoplasmic reticulum stress-induced apoptosis by enhancing DR5 expression in human carcinoma cells, J. Biol. Chem. 279 (2004) 45495–45502, https://doi.org/10.1074/jbc.M406933200.
[37] N. Ohoka, S. Yoshii, T. Hattori, K. Onozaki, H. Hayashi, TRB3, a novel ER stress-inducible gene, is induced via ATF4-CHOP pathway and is involved in cell death, EMBO J. 24 (2005) 1243–1255, https://doi.org/10.1038/sj.emboj.7600596.
[38] S.J. Marciniak, C.Y. Yun, S. Oyadomari, I. Novoa, Y. Zhang, R. Jungreis, K. Nagata, H.P. Harding, D. Ron, CHOP induces death by promoting protein synthesis and oxidation in the stressed endoplasmic reticulum, Genes Dev. 18 (2004) 3066–3077, https://doi.org/10.1101/gad.1250704.
[39] X. Xu, J.G. Park, J.S. So, A.H. Lee, Transcriptional activation of Fsp27 by the liver-enriched transcription factor CREBH promotes lipid droplet growth and hepatic steatosis, Hepatology 61 (2015) 857–869, https://doi.org/10.1002/hep.27371.
[40] J.S. Lee, R. Mendez, H.H. Heng, Z.Q. Yang, K. Zhang, Pharmacological ER stress promotes hepatic lipogenesis and lipid droplet formation, Am. J. Transl. Res. 4 (2012) 102–113.